Available online at www.sciencedirect.com
ScienceDirect
Pharmacology, Biochemistry and Behavior 85 (2006) 464–473
PHARMACOLOGY BIOCHEMISTRY AND BEHAVIOR
www.elsevier.com/locate/pharmbiochembeh

Nociceptive stimulus modality-related difference in pharmacokinetic–pharmacodynamic modeling of morphine in the rat

Gang-Wei Shang [a,1], Dan-Na Liu [a,1], Lai-Hong Yan [b], Xiu-Yu Cui [b], Kui-Ping Zhang [c], Chao Qi [c], Jun Chen [a,b,*]

[a] *Institute for Biomedical Sciences of Pain and Institute for Functional Brain Disorders, Tangdu Hospital, Fourth Military Medical University, Xi'an 710038, P.R. China*
[b] *Institute for Biomedical Sciences of Pain, Capital University of Medical Sciences, Beijing 100069, P.R. China*
[c] *Nhwa Brain Bio-Med-Pharma Co., Ltd. (Shaanxi), Xi'an 710015, P.R. China*

Received 23 February 2006; received in revised form 18 September 2006; accepted 26 September 2006
Available online 27 November 2006

Abstract

Pharmacokinetics (PK)–pharmacodynamics (PD) modeling, the mathematical description of the relationship between PK and PD, can estimate and predict relevant parameters associated with onset, magnitude and time courses of dose–concentration–effect of a drug. In this report, we introduce a new nonsteady-state and time-dependent PK–PD modeling of a single dose of morphine in which time courses of concentration of unconjugated and estimated conjugated morphine in compartments of either plasma or biophase (cerebrospinal fluid, CSF) and multiple anti-nociceptive effects across thermal and mechanical stimulus modalities in rats were studied. The results showed that: (1) both intragastric and intraperitoneal administration of a single dose of morphine resulted in a differential anti-nociceptive effect in both magnitude and time course of the drug between thermal and mechanical painful stimuli (anti-mechanical pain effect was 2–3 fold stronger than anti-thermal pain effect, $P < 0.01$); (2) the PK data showed that the area under concentration–time curves of conjugated morphine was 4.5 and 2.0 fold bigger than unconjugated morphine in either plasma and biophase compartments, suggesting that the PK processes of unconjugated morphine are different from that of conjugated morphine; (3) the PD data also showed a change in PD characteristics of unconjugated and conjugated morphine across systemic and biophasic compartments for anti-mechanical pain effect, while there was no change at all for anti-thermal pain effect; (4) the difference in analgesia of a single dose of morphine across thermal and mechanical stimulus modalities was well reflected by the difference in the nonsteady-state and time-dependent PK–PD modeling, namely, the clockwise hysteresis loop model well represents the relationship of the time course between unconjugated/conjugated morphine concentration (both plasma and biophase) and anti-thermal pain effect, while the counter-clockwise hysteresis loop model well represents that between conjugated morphine concentration (mainly in biophase) and anti-mechanical pain effect. Taken together, the multiple PD–PK modeling is more useful in estimation and prediction of onset, magnitude and time courses of concentration–multiple pharmacological effects of morphine than simple PK or PD models, and establishment of various multiple PD–PK modeling might also be more useful in optimizing clinical use of existing drugs as well as new drugs for analgesia or treatment of other diseases.

Keywords: Unconjugated morphine; Conjugated morphine; High performance liquid chromatography; Pharmacokinetic–pharmacodynamic modeling; Anti-nociception; Thermal pain response; Mechanical pain response

1. Introduction

Pharmacokinetics (PK) is referred to as a science associated with processes of absorption, distribution, metabolism and elimination of a drug in the body, while pharmacodynamics (PD) is associated with the study of quantitative relationship of dose–concentration responses of a drug. PK–PD modeling, the mathematical description of the relationship between PK and

* Corresponding author. Institute for Biomedical Sciences of Pain and, Institute for Functional Brain Disorders, Fourth Military Medical University, #1 Xinsi Road, Baqiao, Xi'an 710038, P.R. China. Tel.: +86 29 84777942; fax: +86 29 84777945.
E-mail addresses: junchen@fmmu.edu.cn, chenjun@ccmu.edu.cn (J. Chen).
[1] These authors equally contributed to the work.

0091-3057/$ - see front matter © 2006 Elsevier Inc. All rights reserved.
doi:10.1016/j.pbb.2006.09.016

PD, can estimate and predict relevant parameters associated with onset, magnitude and time courses of dose–concentration–effect of a drug (Perez-Urizar et al., 2000). The use of PK–PD modeling is of particular importance to optimize drug use by designing rational dosage forms and dosage regimes in clinical pharmacology and pharmaceutical industry.

Morphine is one of the most effective and well-established clinical analgesics and it has two major conjugated forms of metabolite: morphine-6-glucuronide (M-6-G) and morphine-3-glucuronide (M-3-G) *in vivo* (Kalso et al., 1999a,b; Lotsch, 2005a,b; Dickenson and Kieffer, 2006; Schug and Gandham, 2006). M-6-G has been demonstrated to be more potent than its parent compound in analgesia, whereas M-3-G has been believed not to be effective in analgesia but involved in antagonism to morphine-induced analgesia (Shimomura et al., 1971; Yoshimura et al., 1973; Pasternak et al., 1987; Abbott and Palmour, 1988; Paul et al., 1989; Sullivan et al., 1989; Smith et al., 1990; Gong et al., 1991; Frances et al., 1992; Jurna et al., 1996; Hasselström et al., 1996; Ouellet and Pollack, 1997; Lotsch, 2005a). Although simple PK or PD characteristics of morphine and its metabolites have been well determined respectively in blood (Huwyler et al., 1995; Lotsch et al., 1996; Ouellet and Pollack, 1997; Di Marco et al., 1998; Projean et al., 2003; Edwards and Smith, 2005), cerebrospinal fluid (CSF) (Okura et al., 2003; Payne et al., 1996) and brain extracellular fluid (ECF) (Ekblom et al., 1992; Gardmark and Hammarlund-Udenaes, 1998; Bouw et al., 2000, 2001; Xie et al., 2000), so far there has been no study tightly associating the establishment of a PK–PD modeling of morphine with multiple anti-nociceptive effects across thermal and mechanical stimulus modalities. Over the past twenty years, it has been evident that morphine-induced analgesia through systemic, intrathecal and intracerebral administration is mediated separately by descending noradrenergic and serotonergic systems between mechanical and thermal painful stimulus modalities (Kuraishi et al., 1983, 1985; Giordano and Barr, 1987, 1988). However, no report has been available and directly showing a nociceptive stimulus modality-related difference in PK–PD modeling of morphine in the rat. Therefore, in the present report, we introduce a new nonsteady-state and time-dependent PK–PD modeling of a single dose of morphine in which time course relationship of concentration of the unconjugated and estimated conjugated morphine in compartments of either plasma or biophase (cerebrospinal fluid, CSF) and multiple anti-nociceptive effects across thermal and mechanical stimulus modalities was studied.

2. Materials and methods

2.1. Animals

The experiments were performed on Sprague–Dawley male albino rats weighing from 180 to 250 g. The animals were provided by the Laboratory Animal Center of Fourth Military Medical University (FMMU) and use of the animals was reviewed and approved by the FMMU Animal Care and Use Committee. The present study was carried out in accordance with the National Institute of Health Guide for the Care and Use of Laboratory Animals (NIH Publications No. 80–23) revised 1996 or the UK Animals (Science Procedures) Act 1986 and associated guidelines, or the European Communities Council Directive of 24 November 1986 (86/609/EEC). The guidelines of International Association for the Study of Pain (IASP) for experimental pain research in conscious animals were followed (Zimmermann, 1983). The animals were housed in plastic boxes in groups of 4–6 at 22–26 °C with food and water available *ad libitum* in the colony room. A 12:12 h light dark cycle with lights on at 08:00 was maintained and testing was done between 9:00 and 18:30. The rats were acclimated to the test boxes and slight restraint for at least 30 min each day for 5 days before testing. The rats were randomly divided into four groups: (1) Control group: rats without any treatment ($n=18$); (2) Saline group: rats were only treated with normal physiological saline (0.9% NaCl) ($n=36$); (3) i.g. Morphine group: rats were treated with morphine through oral gavage or intragastric administration (15.0 mg/kg) ($n=146$); (4) i.p. Morphine group: rats were treated with morphine through intraperitoneal administration (6.0 mg/kg) ($n=80$).

2.2. Drugs

Morphine hydrochloride (mol. wt. 375.85) was purchased from the First Pharmaceutical Factory (Shenyang, China), β-D-glucuronide glucuronosohydrolase (EC 3.2.1.31, from *Escherichia coli*) and sulfatase (type H-1, EC 3.1.6.1) were purchased from Sigma Chemical Co. (St. Louis MO, USA), metronidazole (mol. wt. 171.16) was obtained from the Institute of Pharmaceutical Industry (Shaanxi, China).

2.3. Behavioral assay of pain sensitivity

2.3.1. Quantitative measurement of thermal pain sensitivity

Thermal pain sensitivity of rats was determined by paw withdrawal thermal latency (PWTL, s). As described previously (Chen et al., 1999), the rat was placed on the surface of a 2 mm thick glass plate covered with a plastic chamber (20 × 20 × 25 cm), the latency of paw withdrawal reflex to heat stimuli was measured by TC-1 radiant heat stimulator (new generation of RTY-3 made in Xi'an Bobang Technologies of Chemical Industry Co. Ltd., PR China). The distance between the projector lamp bulb (150 W) and the lower surface of the glass floor was adjusted to produce a light spot on the floor surface with 5 mm diameter. Twenty percent of light intensity was adopted as output because for most of the rats tested the PWTL was around 12 s (Chen et al., 1999). The heat stimulus was directed onto posterior surface of one hind paw. Four stimuli were repeated to the same site and the latter three values were averaged as mean PWTL. The inter-stimulus interval was more than 10 min at the same region, 5 min at the different region. The thermal latency was determined as the duration from the onset of heat stimulus to the occurrence of a hind paw withdrawal reflex. The stimulus was stopped if the latency exceeded 30 s so as to avoid excessive tissue injury and the region was considered to be completely unresponsive (for details see Chen et al., 1999). The time

course of anti-nociceptive effect of morphine on thermal pain sensitivity was observed at 0, 15, 30, 45, 60, 90, 120, 180, 240, 300, 360 min after drug or vehicle administration.

2.3.2. Quantitative measurement of mechanical pain sensitivity

Mechanical pain sensitivity of rats was determined by paw withdrawal mechanical threshold (PWMT, mN) in response to mechanical stimuli produced by ascending graded individual von Frey monofilaments with bending forces of 21.07, 27.44, 34.30, 44.10, 53.90, 76.44, 107.80, 147.00, 196.00, 245.00, 294.00, 343.00, 392.00, 441.00, 490.00, 588.0 mN. The rat was placed on a metal mesh floor covered with the same plastic box and von Frey filaments were applied from underneath the metal mesh floor to the testing site of the target hind paw. The bending force value of the von Frey filament that caused a 50% occurrence of paw withdrawal reflex by 10 times (once every several seconds) stimuli was expressed as the PWMT (for details see Chen et al., 1999). The time course for measurement of mechanical sensitivity was in accord with that of the thermal sensitivity as described above. The time course of anti-nociceptive effect of morphine on mechanical pain sensitivity was observed at 0, 15, 30, 45, 60, 90, 120, 180, 240, 300, 360 min after drug or vehicle administration.

To avoid inter-experimenter differences and subjective bias, all the behavioral observations were performed by one who was blind to the treatment of either vehicle or drug.

2.4. Determination of morphine concentration

2.4.1. Instrumentation and chromatographic conditions

High performance liquid chromatography (HPLC) was performed by using Shimadzu LC-10A chromatographic system which consisted of an LC-10ATVP intelligence pump, a SPD-10AVP UV detector, a SCL-10AVP system controller, a SIL-10ADVP auto injector and a CLASS-VP5.032 chromatographic workstation (Shimadzu, Japan). The mobile phase consisted of acetonitrile–water–phosphoric acid–diethylamine (10:90:0.15:0.25) (v/v/v/v) with a flow rate of 1.2 ml/min (Huwyler et al., 1995; Projean et al., 2003; Edwards and Smith, 2005). It was filtered by a vacuum filter system equipped with a 0.8 μm filter and was degassed by ultrasonic treatment. The analytical column was Phenomenex® C_{18} (150 mm × 4.6 mm, 5 μm). The run-time was 12 min and wave length of the ultraviolet (UV) detection was set at 240 nm.

2.4.2. Preparation of stock, calibration standard and quality control standard solutions

Stock solution of morphine was prepared by dissolving 10 mg morphine hydrochloride in 1.0 ml 0.9% NaCl solution (10,000 μg/ml). The stock internal standard (I.S.) solution was prepared by dissolving 0.1055 mg metronidazole in 10.0 ml 0.9% NaCl solution (1055.0 μg/ml). The different stock solutions were diluted to a series of solutions successively before daily use. All solutions were stored in dark place at −4 °C.

Calibration standard and quality control (QC) standard solutions for unconjugated or total morphine were prepared respectively on the experimental day. Serial dilutions for both unconjugated (ranging from 31.25 to 62,500.00 μg/L) and total (ranging from 50.00 to 50,000.00 μg/L) morphine were prepared with 11 or 10 nominal concentrations, respectively. Lower, middle and upper limits of quantitation for QC standard solutions were 31.25, 625.00, 62,500.00 μg/L for unconjugated and 50.00, 1000.00, 50,000.00 μg/L for total morphine. Linear calibration curves were constructed by plotting the values obtained from: peak-area of morphine measured/peak-area of I.S. in either blank serum or artificial CSF spiked with I.S. and morphine or plasma and CSF samples collected from the rats receiving either i.g. (15 mg/kg) or i.p. (6.0 mg/kg) administration of morphine. Linearity of the calibration graph was shown by coefficient of linearity regression ($R^2 = 0.9999$ for unconjugated, $R^2 = 0.9986$ for total) (method for details see (Projean et al., 2003; Edwards and Smith, 2005).

2.4.3. Blood and CSF sample preparation

To get understanding about the relationship between systemic or biophasic concentration and differential effects of morphine across stimulus modality-related pain responses, both blood and CSF samples were analyzed in a chronological order. Because there are two forms of morphine *in vivo*, namely unconjugated and conjugated, the relationship between concentration of the two forms of morphine and anti-nociceptive effects was also studied in a parallel manner.

Unconjugated morphine was extracted by using a bath extraction method (Shang et al., 1997). A volume of 0.50 ml of blood sample or 0.2 ml of CSF sample spiked with 50 μl of metronidazole (I.S.) was incubated in a water bath at 90 °C for 5 min followed by a Vortex-mix and centrifugation (3000 r/min, 15 min). A volume of 20 μl of obtained supernatant was directly fed into the HPLC system for analysis.

Conjugated forms of morphine (M-3-G and M-6-G) were estimated by subtracting the unconjugated form by the total morphine. Total morphine was obtained *in vitro* by incubation of the same volume of samples with 1000 U β-glucuronidase plus 25 U sulfatase at 37 °C for 120 min according to the method of previous report (Di Marco et al., 1998). Following deconjugation of glucuronides, the analyte was subjected to the same procedure as afore-mentioned.

To evaluate the enzymatic hydrolysis effectiveness, selective deconjugation studies were performed by glucuronidase for enzymatic synthesis of glucuronides. Glucuronidation of morphine was performed with 62,500.00 μg/L drug and incubated as described above. After the incubation period, the conjugation reaction was stopped through a 30 min centrifugation (3000 r/min). An aliquot of this supernatant (0.5 ml) was incubated for 120 min at 37 °C with: (1) no enzyme; (2) 1000 U β-glucuronidase plus 25 U sulfatase. Morphine and its derivatives were extracted with a water bath (90 °C) for 5 min followed by centrifugation (3000 r/min) for 15 min. A volume of 20 μl of the supernatant was directly fed into the HPLC system for analysis.

The validity of the assays used for determination of the unconjugated and total morphine from animal blood and CSF was well approved. The retention time of the absorbent peaks of the blood and CSF samples was 3.15 min and 3.53 min for I.S. and 9.36 min and 10.82 min for morphine, respectively.

Comparing the drug-free with the I.S.-free blank serum, there was no interfering peaks observed in both of the above two types of samples.

2.4.4. Assay validation

The limit of quantitation (LOQ) was determined as the minimum concentration that could be accurately and precisely quantified (lowest data point of the standard curve). The limit of detection (LOD on column) was defined as the amount that could be detected with a signal-to-noise ratio of 3.0. The specificity of the assay for the analytes versus endogenous substances in the matrix was assessed by comparing the lowest concentration in the calibration curves with reconstitutions prepared with drug-free and I.S.-free blank serum or CSF ($n=6$ rats for each types of samples). Accuracy and precision were determined by recovery and reproducibility of the assay, the former was represented by % nominal concentration of the mean measured morphine (mean of measured/nominal × 100%), while the latter was determined by percent coefficient of variation (%CV = standard deviation of mean of measured/mean of measured × 100%). The within-day and between-day accuracy and precision of the assay were determined by using QC standard solution. Within-day precision was determined by analyzing replicate aliquots of QCs ($n=6$/each concentration) on the same day, while between-day precision was determined by repetitive analysis of QC samples ($n=3$) on 3 consecutive days. The values of % nominal concentration ranging 95.00–105.00% and those of %CV < 5% (within-day) or < 10% (between-day) were accepted.

2.5. Experimental design

Following quantitative measurement of baseline PWTL or PWMT, rats were administered with a single dose of morphine through either i.g. (15.0 mg/kg in 0.5 ml saline) or i.p. (6.0 mg/kg in 0.5 ml saline) route. Rats were avoided getting access to excessive food and water or taking any other medicine before and during the study. Blood or CSF samples were collected at 0, 15, 30, 45, 60, 90, 120, 180, 240, 300, 360 min after administration based upon the method of a previous report (Sheng, 1999). After the rat was well anesthetized by i.p. sodium pentobarbital (30 mg/kg), blood sampling was performed by needle puncture of the left heart ventricle and 2 ml of blood was collected with heparinized tube from each rat. For collection of CSF samples, the anesthetized rat was fixed on stereotaxic instrument and 0.2 ml CSF sample was obtained from left lateral ventricle through 50 μl microsyringe following slower perfusion of artificial CSF into right lateral ventricle according to the coordinate (Bregma −0.96 mm, mediolateral 1.6 mm, depth 3.8 mm) (Paxinos and Watson, 2005). The centrifuged blood or CSF samples were stored at −20 °C until HPLC analysis.

2.6. Pharmacokinetic–pharmacodynamic parametric estimates analysis

Pharmacodynamic parametric estimates were represented by AUE (area under the effect versus time curve), E_{max} (% maximum possible effect, %MPE = PWTL or PWMT − baseline/cutoff value − baseline × 100%), T_{max} (the onset of maximal effect) and

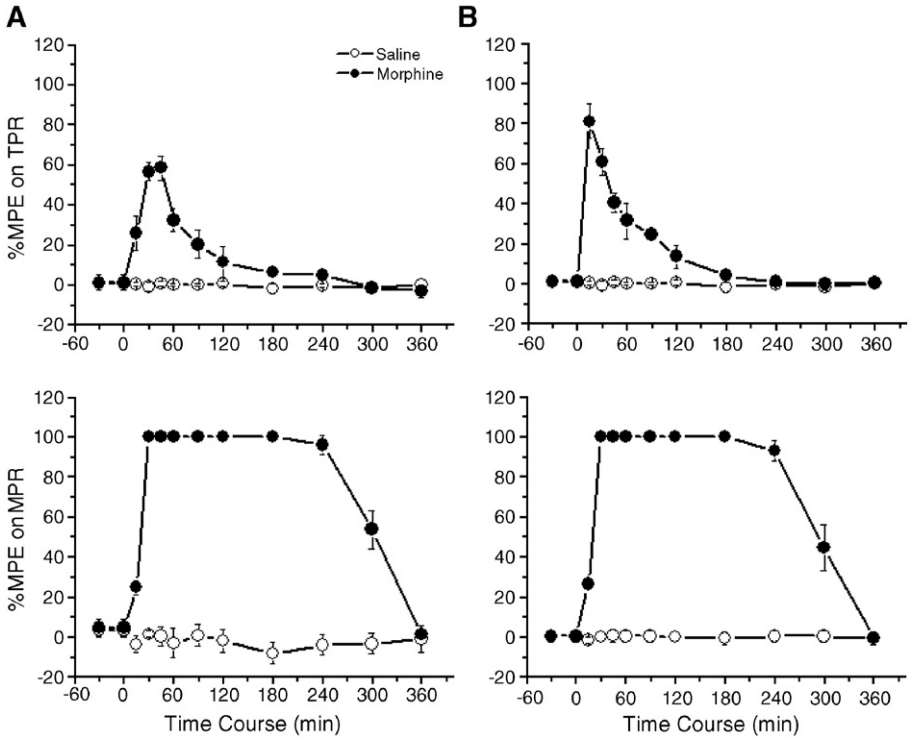

Fig. 1. % maximum possible effect (%MPE) over time course of a single dose of morphine on thermal pain response (TPR, upper panels of A and B) and mechanical pain responses (MPR, lower panels of A and B) following intragastric (i.g., 15.0 mg/kg) or intraperitoneal (i.p., 6 mg/kg) administration.

EC50 (the concentration of half maximal effect). Pharmacokinetic parametric estimates were represented by AUC (area under the concentration versus time curve), C_{max} (maximal concentration) and T_{max} (the time when the maximal concentration reached). The pharmacokinetic and pharmacodynamic parametric estimates were mainly determined by NDST-21, the most commonly used professional software in the field of pharmacology and pharmaceutics in China (New Drug Statistical Treatment-21 or NDST. Ver. 6.0, 1996.6.6 copyright reserved), which was provided by the Chinese Society of Mathematical Pharmacology. NDST-21 requires to be processed under UCDOS (but compatible with Windows 95, Windows 98/Windows Me, Windows NT 4.0, Windows 2000 and Windows XP) and it has been recently updated and renamed as Drug and Statistics (DAS version 2.0) (Huang and Li, 2005) (for more details please refer to: http://www.drugchina.net/das/aboutDAS.asp). Based upon the NDST-21 analysis software, the data for unconjugated morphine from both blood and CSF samples following i.g. administration were analyzed by one-compartment open model, while that for conjugated morphine were analyzed by two-compartment open model (Table 2).

2.7. Data analysis

All data were expressed by mean±SEM. Statistical analyses were performed with SPSS 11.5 statistical software. Comparisons between different groups in each study were performed using non-parametric Mann±Whitney U test. P value <0.05 was considered to be statistically significant.

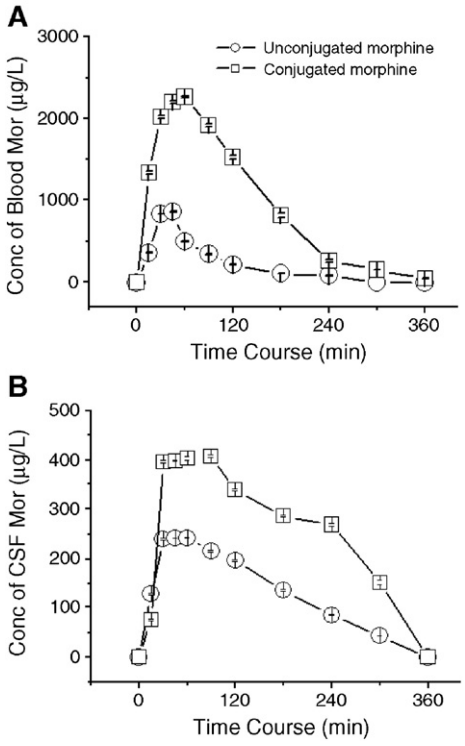

Fig. 2. Concentration–time curves of unconjugated and conjugated morphine from both blood and cerebrospinal fluid (CSF) samples following intragastric administration of a single dose of morphine (15.0 mg/kg). Conc of blood Mor, concentration of blood morphine; Conc of CSF Mor, concentration of CSF morphine.

3. Results

3.1. Differential anti-nociceptive effects of morphine on thermal and mechanical pain responses

Following either i.g. or i.p. administration, morphine produced a robust elevation of pain threshold over the baseline values in response to both radiant heat and von Frey filament mechanical stimuli applied to the rat hind paw (Fig. 1). However, when comparing the effect–time (ET) curves of morphine across stimulus modality-related pain responses, differential anti-nociceptive effects were revealed across thermal and mechanical stimuli following either i.g. or i.p. route of administration (Fig. 1A and B). The steady-state of %MPE on mechanical pain response lasted for 4 h, while that on thermal pain response only lasted for 5–15 min (Fig. 1). When comparing the T_{max}, the onset of maximal effect of anti-mechanical pain effect was about 5 min (for i.g.) or 15 min (for i.p.) slower than that of anti-thermal pain effect (Fig. 1 and Table 1). Moreover, there was a statistically significant difference in AUE between anti-mechanical and anti-thermal pain effects following both i.g. and i.p. administration ($P<0.01$, for both routes of administration), namely, the former was more than 2–3 folds of the latter. This differential effect of morphine could also be reflected by the E_{max}, for which the %MPE on mechanical pain response was nearly 20% (for i.p.) or 40% (for i.g.) higher than that on thermal pain response (Table 1).

Table 1
Pharmacodynamic parametric estimates obtained by NDST-21 analysis of a single dose of i.g. or i.p. morphine in rats[a]

	Morphine (15.0 mg/kg, i.g.)		Morphine (6.0 mg/kg, i.p.)	
	Thermal sensitivity[b]	Mechanical sensitivity[c]	Thermal sensitivity	Mechanical sensitivity
Pharmacodynamic data				
AUE (% μg/L)[d]	8326.68±691.25	27,690.74±1081.94**	7394.47±408.42	28,166.43±2002.09**
E_{max} (%)[e]	58.51±5.98	100.00	81.06±8.46	100.00
T_{max} (min)[f]	30–45 (40.00±3.46)	30–60 (45.00±6.00)	15–30 (17.5±2.74)	30–45 (32.50±2.74)
No. of animals	6	6	6	6

Notes: [a]Data presented as mean±S.E.M.; [b]Thermal sensitivity was determined by paw withdrawal thermal latency (PWTL, s); [c]Mechanical sensitivity was determined by paw withdrawal mechanical threshold (PWMT, mN); [d]AUE was determined as area under the effect versus time curve; [e]E_{max} was % maximum possible effect (PWTL or PWMT-baseline/cutoff value−baseline×100%); [f]T_{max} was determined as the onset of maximal effect; **$P<0.01$: significant difference in pharmacodynamic data between drug effect on thermal and mechanical sensitivity; i.g., oral gavage; i.p., intraperitoneal.

Table 2
Comparison of pharmacokinetic parametric estimates between blood and cerebrospinal fluid samples in one-compartment or two-compartment open model following a single dose of i.g. morphine in rats by NDST-21 analysis[a]

	One-compartment open model for unconjugated morphine		Two-compartment open model for conjugated morphine	
	Blood	CSF	Blood	CSF
AUC (min μg/L)[b]	73,516.70±558.29	44,797.80±323.21**	326,885.80±558.34††	92,095.12±120.86** ††
C_{max} (μg/L)[c]	861.61±2.95	242.10±3.06**	2259.00±12.71††	407.80±8.03** ††
T_{max} (min)[d]	45.00	55.00±3.46†	60.00	80.00±6.93†
EC_{50}(μg/L)				
Anti-thermal pain effect	499.00±80.42	242.10±39.80	2196.89±804.22	403.87±26.39
Anti-mechanical pain effect	361.33±6.66	128.50±6.66	1334.67±439.38	103.32±17.06
No. of animals	6	6	6	6

Notes: [a]Data presented as mean±S.E.M.; [b]AUC was determined as area under the concentration versus time curve; [c]C_{max} was maximal concentration; [d]T_{max} was determined as the time when the maximal concentration reached; [e]EC_{50} was the concentration of half maximal effect of a single dose of morphine (15.0 mg/kg). **$P<0.01$: significant difference in AUC and C_{max} values between blood and cerebrospinal fluid (CSF) samples following i.g. administration of drug; ††$P<0.01$: significant difference in AUC and C_{max} values between unconjugated and conjugated morphine in either blood or CSF samples following i.g. administration; †$P<0.01$: significant difference in T_{max} values of either unconjugated or conjugated morphine between blood and CSF samples following i.g. administration of drug; i.g., oral gavage.

3.2. PK or PD data

3.2.1. Comparison of the PK data between plasma and biophase compartments

Fig. 2 shows concentration–time (CT) curves for both blood and CSF samples. Based upon the CT curves, the unconjugated and the estimated conjugated morphine were compared and there was a significant difference in the values of AUC for both blood and CSF samples (Fig. 2 and Table 2). As for the blood samples, the values of AUC and C_{max} of the conjugated morphine were about 4.5 and 2.6 fold larger than those of the unconjugated form (††$P<0.01$), while as for the CSF samples the values of the conjugated morphine were 2.0 and 1.7 fold larger than those of the unconjugated form (**$P<0.01$, Fig. 2 and Table 2). There was also a 10–20 min delay in the T_{max} values between blood and CSF samples (Fig. 2 and Table 2).

3.2.2. Comparison of the PD data between plasma and biophase compartments

As shown in Fig. 3, the effect–concentration (EC) curves for %MPE on thermal pain response in both blood and CSF samples were linear for both unconjugated and conjugated morphine (Fig. 3A). As for %MPE on mechanical pain response, however, the EC curves in both blood and CSF samples were typically

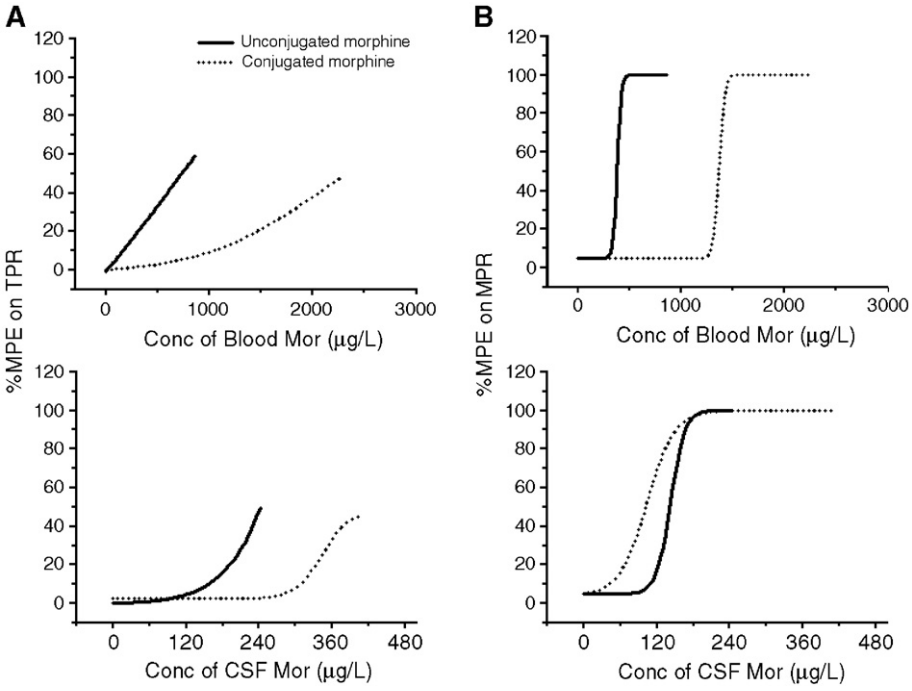

Fig. 3. The relationship between concentration and effects of unconjugated and conjugated morphine from blood and cerebrospinal fluid (CSF) samples across thermal and mechanical pain responses following intragastric administration of a single dose of morphine (15.0 mg/kg). %MPE on TPR or %MPE on MPR, percent maximum possible effect on thermal pain response or mechanical pain response; Conc of blood Mor, concentration of blood morphine; Conc of CSF Mor, concentration of CSF morphine.

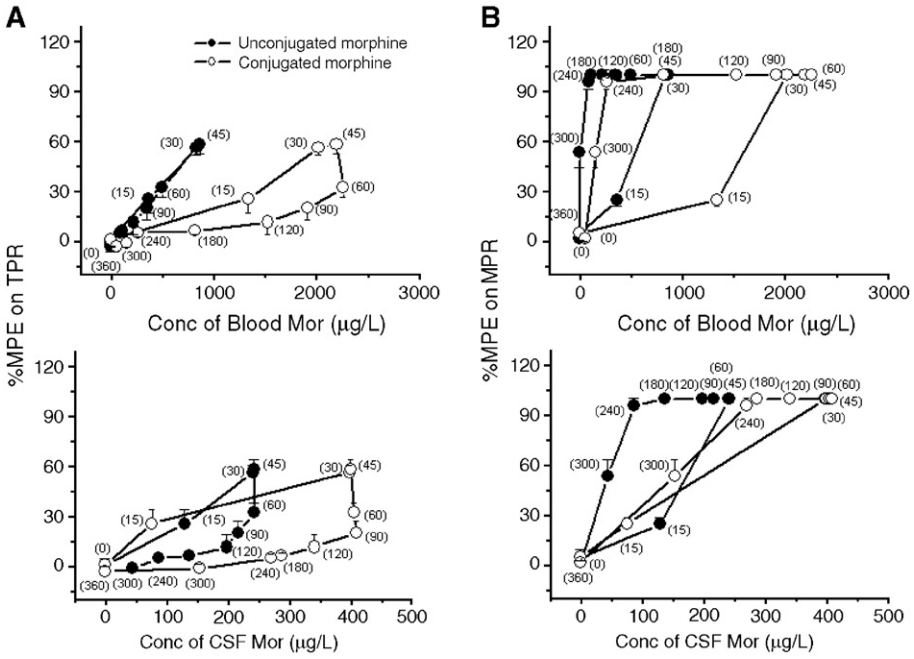

Fig. 4. Modes of effect–concentration–time (ECT) curves (hysteresis loop plottings) of unconjugated and conjugated morphine from blood and cerebrospinal fluid (CSF) across thermal and mechanical pain responses. %MPE on TPR or %MPE on MPR, percent maximum possible effect on thermal pain response or mechanical pain response; Conc of blood Mor, concentration of blood morphine; Conc of CSF Mor, concentration of CSF morphine; the numerical data in the parenthesis are time points for collection of blood or CSF samples from rats receiving intragastric administration of a single dose of morphine (15.0 mg/kg).

hyperbolic for both unconjugated and conjugated morphine (Fig. 3B). Moreover, it was surprisingly noted that the positions of the EC curves for unconjugated and conjugated morphine were different from each other across blood and CSF samples for anti-mechanical pain effect, while those for anti-thermal pain effect were not changed. As shown in Fig. 3B, the EC curve of unconjugated morphine in blood was far leftward to that of conjugated morphine, while that of unconjugated morphine in CSF was switched to the rightward to the conjugated form of morphine.

3.3. Differential models of effect–concentration–time curves of morphine across thermal and mechanical pain responses

To see whether there is a change in models of effect–concentration–time (ECT) curves of unconjugated and conjugated morphine across thermal and mechanical pain responses following a single dose of morphine, hysteresis loops were plotted based upon the nonsteady-state and time-dependent conditions of the present data. As shown in Fig. 4A and B, the ECT loop plotting for anti-thermal pain effects of unconjugated morphine in either blood or CSF samples was represented as a clockwise hysteresis model in which the relationship between the concentration and effect was highly correlated over the whole time course including both the rising phase and the falling phase of the loop (Fig. 4A). However, in sharp contrast, the ECT loop plotting for anti-mechanical pain effects of unconjugated morphine in either blood or CSF samples was represented as a counter-clockwise hysteresis model in which the relationship between the concentration and effect was correlated over the time course of the rising phase, but not the falling phase, of the hysteresis loop (Fig. 4B). As for the properties of the ECT loop plotting of conjugated morphine, the clockwise hysteresis model well represented the modes of anti-thermal pain effect, while the counter-clockwise hysteresis model well represented the modes of anti-mechanical pain effect in both systemic and biophasic compartments. Nonetheless, the relationship between the concentration and effect was not correlated over the time course of the falling phase although the correlative relationship was likely remained unchanged over the time course of the rising phase of both clockwise and counter-clockwise hysteresis loops (Fig. 4A and B). When further looking insight into the falling phase of the hysteresis loops, it was surprisingly found that the long-lasting steady-state anti-mechanical pain effects of a single dose of morphine was mainly caused by the long-term higher concentration of conjugated morphine in CSF (over 250–400 μg/L for 30–240 min), but not by conjugated morphine in blood or unconjugated morphine in blood and CSF (Fig. 4B).

4. Discussion

4.1. Nociceptive stimulus modality-related difference in PK–PD modeling of a single dose of morphine

PK–PD modeling is generally divided into two classes: (1) steady-state and time-invariant PK–PD models which can be used under constant concentration of the active moiety at the action site following long-term infusion or multiple doses of a drug; (2) nonsteady-state and time-variant (or time-dependent) PK–PD models which can be used when the time courses of concentration and effect are out of phase following a single dose of a drug or when time-dependent changes in PD parameters are

present (Perez-Urizar et al., 2000). In the present study, it was found that a single dose of morphine resulted in a distinct dissociation of the time courses of anti-nociceptive effect across thermal and mechanical stimulus modalities. The nociceptive stimulus modality-related difference in time courses of anti-nociceptive effect of a single dose of morphine was well represented by nonsteady-state and time-dependent PK–PD modeling in both systemic (plasma) and biophase (CSF) compartments. It was thus characterized that the fast and short-lasting anti-thermal pain effect of morphine was well represented by clockwise hysteresis model, while the delayed and long-lasting anti-mechanical pain effect of morphine was well represented by counter-clockwise hysteresis model in both plasma and biophase compartments. By comparing the time courses of concentration and anti-nociceptive effect of unconjugated and conjugated morphine between plasma and CSF compartments across thermal and mechanical pain stimuli, it was revealed that there was a distinct difference in the falling phases of the hysteresis loops across the two stimulus modalities, while the rising phases were remained less changed, suggesting that the difference in the hysteresis loops across the thermal and mechanical stimulus modalities should be caused by changes in the falling phases of the hysteresis loops.

It is known that clockwise hysteresis model means that effect of a drug decreases quicker than plasma and site concentration and reflects tolerance phenomenon to the drug induced by desensitization of receptors or production of counterregulatory substances (Perez-Urizar et al., 2000). Because the present results showed that clockwise hysteresis model corresponded to the fast and short-lasting anti-thermal pain effect, we had reason to speculate that tolerance might occur mainly for anti-thermal pain effect, but not for anti-mechanical pain effect, following a single dose of morphine. Moreover, based upon the features of the clockwise hysteresis loops it was shown that both unconjugated and conjugated morphine in biophase compartment as well as conjugated morphine in plasma might be involved in morphine tolerance for anti-thermal pain effect. This finding might have significant implications for the future study of morphine tolerance.

Also as suggested by Perez-Urizar et al. (2000), under nonsteady-state condition, the dissociation of time courses of concentration and effect might be caused by disequilibrium between biophase and plasma compartments, delayed appearance of active metabolites interacting at the same receptors as parent compound, indirect mechanisms of action (inhibition or stimulation of the synthesis or degradation of endogenous substances), etc. The PK–PD modeling of anti-mechanical pain effect of a single dose of morphine showed a distinct difference in the falling phases of the counter-clockwise hysteresis loops between plasma and biophase compartments for the conjugated morphine, while there was no difference between the plasma and biophase compartments for unconjugated morphine. As a consequence, the long-lasting steady-state anti-mechanical pain effects of a single dose of morphine was likely caused by the long-term higher concentration of conjugated morphine in biophase, but not by conjugated morphine in plasma or unconjugated morphine in either plasma or biophase compartments and this was partially consistent with previous reports showing long-lasting anti-nociceptive effect of M-6-G in Brain ECF (Ekblom et al., 1992; Gardmark and Hammarlund-Udenaes, 1998; Bouw et al., 2000, 2001; Xie et al., 2000). Regarding the mechanisms of the delayed and long-lasting anti-mechanical pain effect of morphine, it could be produced by delayed appearance and disequilibrium of conjugated morphine between biophase and plasma compartments, and probably indirect mechanisms of actions of morphine acting at the receptors and these possibilities have been suggested by previous literatures (Ekblom et al., 1992; Gardmark and Hammarlund-Udenaes, 1998; Bouw et al., 2000, 2001; Xie et al., 2000). Moreover, the nociceptive stimulus modality-related differences in PK–PD modeling are also likely to be caused by various localizations of three classes (μ-, δ-, κ-) of opioid receptors in both peripheral and central nervous system of the pain signaling pathways, especially μ-opioid receptors to which morphine has highest affinity resulting in various pharmacological actions (Kalso et al., 1999a,b; Dickenson and Kieffer, 2006). Co-localization of peripheral thermal nociceptors (TRPV1) in small-medium sized primary sensory cells of dorsal root ganglia (DRG) expressing μ-opioid receptors, but not in large sized DRG cells, highly supports the molecular basis of differential anti-nociceptive effect of morphine across thermal and mechanical pain sensation (Julius and Basbaum, 2001; Julius and McCleskey, 2006).

Another important significance of the present results was that the nociceptive stimulus modality-related difference in PK–PD modeling could predict the relationship between action site and pharmacological actions of a drug. Based upon the features of clockwise and counter-clockwise hysteresis models, the relationship between site concentration and anti-nociceptive effects of morphine could also be estimated by using plasma and biophase compartment models. Because of the existence of the correlative relationship between concentration and anti-nociceptive effects of both unconjugated and conjugated morphine on the rising phases of both clockwise and counter-clockwise hysteresis models across plasma and biophase compartments, it is suggested that both unconjugated and conjugated morphine in plasma and biophase compartments are involved in generation of anti-thermal pain effects and the early phase of anti-mechanical pain effects, however, only conjugated morphine in biophase compartment is involved in generation of the long-lasting phase of anti-mechanical pain effects. The difference in action sites and structural forms of morphine and its metabolites in production of analgesia across thermal and mechanical pain stimulus modalities might be accounted for by previous results showing separate involvement of the spinal noradrenergic and serotonergic systems in anti-mechanical and anti-thermal analgesia of morphine (Kuraishi et al., 1983, 1985, Giordano and Barr, 1987, 1988) and state-dependent opioid control of pain in the CNS (Fields, 2004).

4.2. Clinical implication and significance

As introduced at the beginning of this report, the most useful advantage of PK–PD modeling is that it can estimate and predict relevant parameters associated with onset, magnitude

and time courses of dose–concentration–effect of a drug. The use of PK–PD modeling will be of particular importance in clinical pharmacology and pharmaceutical industry for optimizing drug dosage forms and dosage regimes (Perez-Urizar et al., 2000). However, development of multiple PD–PK modeling of a single dose of a certain drug has been greatly limited due to lack of parallel studies on the relationship between multiple PD and PK. As a good example, the finding of the nociceptive stimulus modality-related difference in PK–PD modeling of a single dose of morphine would lead to opening of a new way for the study of multiple PD–PK modeling of clinical and novel analgesics.

Moreover, because normal pain sensation evoked by thermal and mechanical noxious stimuli can be dramatically enhanced or exaggerated following tissue or nerve injury, resulting in thermal and mechanical hyperalgesia or allodynia (Chen, 2003; Meyer et al., 2006), it is also of particular importance to establish a PK–PD modeling under pathological pain states. Generally, clinical pain or pathological origins of pain consist of two types: (1) nociceptive pain caused by peripheral tissue injury or inflammation; (2) neuropathic pain caused by peripheral or central nerve injury (Merskey and Bogduk, 1994). In clinic, it is widely accepted that pain is not equally sensitive to analgesic drugs and this clinical pharmacological discrepancy for analgesics has long been thought to be caused by inter-individual difference, age, gender, and drug administration routes, etc. However, difference in anti-nociceptive effects of analgesics might also be caused by different stimulus modalities (thermal, mechanical and chemical), as demonstrated in the present study, as well as different pain states (e.g., physiological vs. pathological, inflammatory vs. neuropathic, etc.). With regard to the morphine-induced analgesia, the studies associated with the dose–effect, action sites, routes of administration, receptors, tolerance and side effects (e.g., addiction, respiratory depression and constipation, etc.) have been well conducted (Kalso et al., 1999a,b; Lotsch, 2005a,b; Dickenson and Kieffer, 2006; Schug and Gandham, 2006; Gourlay, 1999). Analgesic effects of morphine and other opioids have also been evaluated in various animal models of inflammatory or neuropathic pain states (Guilbaud et al., 1999; Ossipov et al., 1999; Xu et al., 1999). Both animal and human studies indicate that morphine has analgesic effect under the inflammatory pain state, however it does not produce analgesic effect under some neuropathic pain states (Guilbaud et al., 1999; Ossipov et al., 1999). For example, in both the chronic constriction injury and the L5/L6 ligation model of neuropathic pain, intrathecal morphine could reverse thermal hyperalgesia, but was without anti-nociceptive effects on the tail-flick response or tactile allodynia (Ossipov et al., 1999). This suggests that the anti-nociceptive effects of morphine might also differ among different pathological pain states. The difference in anti-nociception of morphine and other analgesics under different pathological states or in different animal models of pain remains to be further evaluated by using multiple PD–PK modeling.

In summary, in the present study we established a nonsteady-state and time-dependent multiple PD–PK modeling of a single dose of morphine for both plasma and biophase compartments in rats. By using the model profile, the difference in analgesia of a single dose of morphine across different nociceptive stimulus modalities was well reflected by the difference in the PK–PD modeling, namely, the clockwise hysteresis loop model well represents the relationship of the time course between unconjugated/conjugated morphine concentration (in both plasma and biopase) and anti-thermal pain effect, while the counter-clockwise hysteresis loop model well represents that between conjugated morphine concentration (mainly in biophase) and anti-mechanical pain effect. The multiple PD–PK modeling might be useful in estimation and prediction of onset, magnitude and time courses of concentration and multiple pharmacological effects of existing clinical drugs as well as new drugs for analgesia or treatment of other diseases.

Acknowledgements

The work was partially supported by 973 Program (2006CB500800), NSFC grant (30325023), Innovation Research Team Program of MOE (IRT0560), Military Health and Medicinal Program (06G095) and Beijing NSF grant (KZ200510025016) to J. Chen.

References

Abbott F, Palmour M. Morphine-6-glucuronide: analgesic effects and receptor binding profile in rats. Life Sci 1988;43:1685–95.

Bouw MR, Gardmark M, Hammarlund-Udenaes M. Pharmacokinetic–pharmacodynamic modeling of morphine transport across the blood–brain barrier as a cause of the antinociceptive effect delay in rats — a microdialysis study. Pharm Res 2000;17:1220–7.

Bouw MR, Xie R, Tunblad K, Hammarlund-Udenaes M. Blood–brain barrier transport and brain distribution of morphine-6-glucuronide in relation to the antinociceptive effect in rats — pharmacokinetic/pharmacodynamic modeling. Br J Pharmacol 2001;134:1796–804.

Chen J. The bee venom test: a novel useful animal model for study of spinal coding and processing of pathological pain information. In: Chen J, Chen CAN, Han JS, Willis WD, editors. Experimental pathological pain: from molecules to brain functions. Beijing: Science Press; 2003. p. 77-110.

Chen J, Luo C, Li HL, Chen HS. Primary hyperalgesia to mechanical and heat stimuli following subcutaneous bee venom injection into the plantar surface of hindpaw in the conscious rat: a comparative study with the formalin teat. Pain 1999;83:67–76.

Di Marco MP, Felix G, Descorps V, Ducharme MP, Wainer IW. On-line deconjugation of glucuronides using an immobilized enzyme reactor based upon β-glucuronidase. J Chromatogr B 1998;715:379–86.

Dickenson A, Kieffer B. Opiates: basic mechanisms. In: MacMahon SB, Koltzenburg M, editors. Wall and Melzack's textbook of pain. 5th edition. China: Elsevier Churchill Livingstone; 2006. p. 427–42.

Edwards SR, Smith MT. Simultaneous determination of morphine, oxycodone, morphine-3-glucuronide, and noroxycodone concentrations in rat serum by high performance liquid chromatography-electrospray ionization-tandem mass spectrometry. J Chromatogr B 2005;814:241–9.

Ekblom M, Gardmark M, Hammarlund-Udenaes M. Estimation of unbound concentrations of morphine from microdialysate concentrations by use of nonlinear regression analysis *in vivo* and *in vitro* during steady state conditions. Life Sci 1992;51:449–60.

Fields H. State-dependent opioid control of pain. Nat Rev Neurosci 2004;5:565–75.

Frances B, Gout R, Monsarrat B, Cros J, Zajac JM. Further evidence that morphine-6 beta-glucuronide is a more potent opioid agonist than morphine. J Pharmacol Exp Ther 1992;262:25–31.

Gardmark M, Hammarlund-Udenaes M. Delayed antinociceptive effect following morphine-6-glucuronide administration in the rat — pharmacokinetic/pharmacodynamic modeling. Pain 1998;74:287–96.

Giordano J, Barr GA. Morphine and ketocyclazocine-induced analgesia in the developing rat: differences due to type of noxious stimulus and body topography. Dev Brain Res 1987;32:247–53.

Giordano J, Barr GA. Effects of neonatal spinal cord serotonin depletion on opiate-induced analgesia in tests of thermal and mechanical pain. Dev Brain Res 1988;41:121–7.

Gong Q, Hedner T, Hedner J, Björkman R, Nordberg G. Antinociceptive and ventilatory effects of the morphine metabolites: morphine-6-glucuronide and morphine-3-glucuronide. Eur J Pharmacol 1991;193:47–53.

Gourlay GK. Different opioid — same actions? In: Kalso E, McQuay HJ, Wiesenfeld-Hallin Z, editors. Opioid sensitivity of chronic noncancer pain. Seattle: IASP Press; 1999. p. 97-115.

Guilbaud G, Kayser V, Perrot S, Keita H. Antinociceptive effect of opioid substances in different models of inflammatory pain. In: Kalso E, McQuay HJ, Wiesenfeld-Hallin Z, editors. Opioid sensitivity of chronic noncancer pain. Seattle: IASP Press; 1999. p. 201–23.

Hasselström J, Svensson JO, Säwe J, Wiesenfeld-Hallin Z, Yue QY, Xu XJ. Disposition and analgesic effects of systemic morphine, morphine-6-glucuronide and normorphine in rat. Pharmacol Toxicol 1996;79:40–6.

Huang XH, Li J, RY SUN, Cheng ZY, Zheng QS. Drug and Statistics Software (DAS), version 2.0. Mathematical Pharmacology Professional Committee of China. 2005. 950 RMB(≈$115 US). Am J Pharm Educ 2005:397–8.

Huwyler J, Rufer S, Kusters E, Drewe J. Rapid and highly automated determination of morphine and morphine glucuronides in plasma by on-line solid-phase extraction and column liquid chromatography. J Chromatogr B 1995;674:57–63.

Julius D, Basbaum AI. Molecular mechanisms of nociception. Nature 2001;413:203–10.

Julius D, McCleskey EW. Cellular and molecular properties of primary afferent neurons. In: MacMahon SB, Koltzenburg M, editors. Wall and Melzack's textbook of pain. 5th edition. China: Elsevier Churchill Livingstone; 2006. p. 35–48.

Jurna I, Baldauf J, Fleischer W. Depression by morphine-6-glucuronide of nociceptive activity in rat thalamus neurons: comparison with morphine. Brain Res 1996;722:132–8.

Kalso E. Route of opioid administration: does it make a difference? In: Kalso E, McQuay HJ, Wiesenfeld-Hallin Z, editors. Opioid sensitivity of chronic noncancer pain. Seattle: IASP Press; 1999a. p. 117–28.

Kalso E, McQuay HJ, Wiesenfeld-Hallin Z. Opioid sensitivity of chronic noncancer pain. Seattle: IASP Press; 1999b.

Kuraishi Y, Harata Y, Aratani S, Satoh M, Takagi H. Separate involvement of the spinal noradrenergic and serotonergic systems in morphine analgesia: mechanical and thermal analgesic tests. Brain Res 1983;273:245–52.

Kuraishi Y, Hirota N, Satoh M, Takagi H. Antinociceptive effects of intrathecal opioids, noradrenaline and serotonin in rats: mechanical and thermal analgesic tests. Brain Res 1985;326:168–71.

Lötsch J. Opioid metabolites. J Pain Symptom Manage 2005a;29:S10–24.

Lötsch J. Pharmacokinetic–pharmacodynamic modeling of opioids. J Pain Symptom Manage 2005b;29:S91-S103.

Lötsch J, Stockmann A, Kobal G, Brune K, Waibel R, Schmidt N, Geisslinger G. Pharmacokinetics of morphine and its glucuronides after intravenous infusion of morphine and morphine-6-glucuronide in healthy volunteers. Clin Pharmacol Ther 1996;60:316–25.

Merskey H, Bogduk N. Classification of chronic pain2nd edition. Seattle: IASP Press; 1994.

Meyer RA, Ringkamp M, Campbell JN, Raja SN. Peripheral mechanisms of cutaneous nociception. In: MacMahon SB, Koltzenburg M, editors. Wall and Melzack's textbook of pain. 5th edition. China: Elsevier Churchill Livingstone; 2006. p. 3-34.

Okura T, Saito M, Nakanishi M, Komiyama N, Fujii A, Yamada S, Kimura R. Different distribution of morphine and morphine-6β-glucuronide after intracerebroventricular injection in rats. Br J Pharmacol 2003;140:211–7.

Ossipov MH, Lai J, Malan TP, Porreca F. Opioid analgesic activity in neuropathic pain states. In: Kalso E, McQuay HJ, Wiesenfeld-Hallin Z, editors. Opioid sensitivity of chronic noncancer pain. Seattle: IASP Press; 1999. p. 163–81.

Ouellet DMC, Pollack GM. Effect of prior morphine-3-glucuronide exposure on morphine disposition and antinociception. Biochem Pharmacol 1997;53:1451–7.

Pasternak GW, Bodnar RJ, Clark JA, Inturrisi CE. Morphine-6-glucuronide, a potent mu agonist. Life Sci 1987;41:2845–9.

Paul D, Standifer KM, Inturrisi CE, Pasternak GW. Pharmacological characterization of morphine-6-beta-glucuronide, a very potent morphine metabolite. J Pharmacol Exp Ther 1989;251:477–83.

Paxinos G, Watson C. The rat brain in stereotaxic coordinates. Amsterdam: Elsevier Academic Press; 2005.

Payne R, Gradert TL, Inturrisi CE. Cerebrospinal fluid distribution of opioid after intra-ventricular and lumbar subarachnoid administration in sheep. Life Sci 1996;59:1307–21.

Perez-Urizar J, Granados-Soto V, Flores-Murrieta FJ, Castaneda-Hernandez G. Pharmacokinetic–pharmacodynamic modeling: why? Arch Med Res 2000;31:539–45.

Projean D, Tu TM, Ducharme J. Rapid and simple method to determine morphine and its metabolites in rat plasma by liquid chromatography-mass spectrometry. J Chromatogr B 2003;787:243–53.

Schug SA, Gandham N. Opioids: clinical use. In: MacMahon SB, Koltzenburg M, editors. Wall and Melzack's textbook of pain. 5th edition. China: Elsevier Churchill Livingstone; 2006. p. 443–57.

Shang GW, Jiang YP, Huang X, Fan YX, Mei QB, He ZG. Determination of free ferulic acid in serum of healthy volunteers after administration of compound Chuanxiong decoctions by RP-HPLC. Chin Pharm J 1997;32:761–4.

Sheng H. A method of gathering blood by intracardiac penetration in living rats. Acta Acad Med Hubei 1999;20:130–1.

Shimomura K, Kamata O, Ueki S, Ida S, Oguri K. Analgesic effect of morphine glucuronides. Tohoku J Exp Med 1971;105:45–52.

Smith MT, Watt JA, Cramond T. Morphine-3-glucuronide — a potent antagonist of morphine analgesia. Life Sci 1990;47:579–85.

Sullivan AF, McQuay HJ, Bailey D, Dickenson AH. The spinal antinociceptive actions of morphine metabolites morphine-6-glucuronide and normorphine in the rat. Brain Res 1989;482:219–24.

Xie R, Bouw MR, Hammarlund-Udenaes M. Modelling of the blood–brain barrier transport of morphine-3-glucuronide studied using microdialysis in the rat: involvement of probenecid-sensitive transport. Br J Pharmacol 2000;131:1784–92.

Xu XJ, Yu W, Hao JX, Hokfelt T, Wiesenfeld-Hallin Z. Opioid sensitivity in experimental central pain after spinal cord injury in rats. In: Kalso E, McQuay HJ, Wiesenfeld-Hallin Z, editors. Opioid sensitivity of chronic noncancer pain. Seattle: IASP Press; 1999. p. 183–200.

Yoshimura H, Ida S, Oguri K, Tsukamoto H. Biochemical basis for analgesic activity of morphine-6-glucuronide-1. Biochem Pharmacol 1973;22:1423–30.

Zimmermann M. Ethical guidelines for investigations of experimental pain in conscious animals. Pain 1983;16:109–10.